

# 双管级联薄管激光放大器环域像差自补偿方法

李佳, 田博宇, 余江川, 张彬\*

四川大学电子信息学院, 四川 成都 610064

**摘要** 针对高功率双管级联薄管激光放大器的环域像差补偿需求, 提出了一种环域像差自补偿方法。该方法通过一个直角锥镜使非理想薄管激光光路折转, 利用往返光路共轭的特性实现畸变波前的自补偿。通过数值模拟仿真, 验证了双管结构中单个薄管引入加工误差及光源对准误差时该自补偿方法的校正能力, 并详细分析了该方法对双管配合误差的自补偿效果。在此基础上, 进一步考虑了直角锥镜误差对双管级联结构波前环域像差补偿效果的影响。结果表明, 该自补偿方法能有效抑制双管级联薄管激光放大器中由加工误差和装调误差所引入的环域离轴像差, 且对直角锥镜装调误差容限较大, 有利于提升薄管激光器的抗失调稳定性。

**关键词** 激光器; 双管级联薄管激光放大器; 直角锥镜; 自补偿; 环域像差

中图分类号 TN248; O436 文献标码志码 A

doi: 10.3788/CJL202148.1301006

## 1 引言

采用“之字形”光路的固态激光器因其轻量化、输出功率高、光束质量好、热稳定性高等优点, 在工业、军事与国防等领域得到广泛应用<sup>[1-5]</sup>。“之字形”光路薄管固态激光器作为一种增益介质为管状结构的新型高功率激光器, 不仅克服了棒状与板条状激光器热负载能力不足的问题, 还具备了结构紧凑、增益体积大以及无边界效应等独特优势, 提供了一种实现高能激光输出的潜在途径<sup>[6-8]</sup>。然而, 高功率固体激光器不可避免地存在热光效应, 容易造成激光器输出功率下降、光束质量劣化等不利影响<sup>[9-11]</sup>。为实现高功率的激光输出, 常用的一种方法是将双管级联以补偿热致退偏效应, 并获得更大的有效增益体积<sup>[12-13]</sup>。同时, 为了进一步提升薄管散热性能以抑制热致波前畸变, 通常将管状增益介质加工成大口径、薄壁窄环构型, 并结合“之字形”光路, 可有效抑制薄管径向温度梯度导致的光束质量退化。

尽管“之字形”光路双管级联能有效提升薄管激光器的输出功率和动态热畸变, 但由于薄管窄环状的特殊构型及薄管内光路反射次数的增多, “之字形”光路薄管固态激光器的静态波前畸变的管控难

度极大。一方面, 管状增益介质可通过沿棒状晶体光轴钻孔加工而成, 但受到加工精度的影响, 这一过程将不可避免地引入同心度、平行度、长度与厚度等多种加工误差。其中, 又以薄管同心度与平行度误差所引起的离轴像差对光束质量的影响最为严重<sup>[14]</sup>。由于管状介质中的“之字形”光路对入射光线方位角极为敏感, 因而光源对准误差也是引起光束质量下降的另一重要因素。另一方面, 双管构型在装配过程中产生的配合误差将进一步加剧光束质量的退化。上述非理想因素均会导致薄管中的光线偏离理想路径, 以略微旋转的方式传输, 最终致使光束质量明显变差<sup>[14]</sup>。此外, 由于薄管激光器输出光束为大遮拦比的窄带环形光束, 传统的自适应校正系统难以完全满足大孔径、薄壁管状介质的像差校正需求<sup>[15]</sup>。因此, 寻求有效的薄管激光环域像差校正方法, 特别是针对环域离轴像差的校正, 是保证薄管光束质量的关键。

Tian 等<sup>[16]</sup>提出了单薄管的光束质量自补偿方法, 该方法是在薄管管状增益介质的一端装配一个直角锥镜元件, 利用内锥面光线平行回射的特性及薄管结构静态共轭光路互补的特性, 实现环域离轴像差的自补偿。然而, 在实际工程应用中, 为了获得

收稿日期: 2020-11-09; 修回日期: 2020-12-28; 录用日期: 2021-02-07

基金项目: 四川省科技计划资助项目(2018JY0553)、中国科学院自适应光学重点实验室基金(LAOF1801)

通信作者: \*zhangbinff@sohu.com

更高的激光输出功率,大多采用多管级联结构<sup>[17-18]</sup>。为此,我们在已有工作基础上,以 Nd : YAG 双管级联薄管放大系统为例,深入研究了基于共轭光路的双管级联薄管激光放大器光束质量校正方法,重点分析了双管级联薄管激光放大器中两薄管分别存在装调误差与加工误差以及双管存在配合误差时,采用该自补偿方法的有效性。进一步讨论了直角锥镜的加工误差与装调误差对光束质量校正作用的影响,并结合环域 Zernike 像差理论,对直角锥镜误差引入的波前像差进行了定量分析。

## 2 理论模型

在实际应用中,由于系统装调不理想及管状介质存在加工误差等问题,会将装调误差与加工误差引入到双管结构中。同时,双管配合误差的存在也将对光束质量产生不利影响。以较为敏感的光源对准误差(光源轴线与薄管轴线的夹角)、同心度误差(薄管内外壁轴线的偏移量)及平行度误差(薄管内外壁轴线的夹角)等静态误差为例,图 1(a)给出了双管级联结构环域像差形成原理示意图。当薄

管激光器存在对准误差  $\Delta\theta_s$ 、同心度误差  $\Delta x$  及平行度误差  $\Delta\theta$  时,环形光束在 XOY 面上的入射位置会偏离理想位置且光束传输路径将沿入射方位角方向发生旋转、会聚或发散,进而引发环域离轴像差,严重影响光束质量<sup>[14]</sup>。图 1(b)为薄管激光器结构示意图,双管级联薄管激光器采用 LD 侧面泵浦结构,对于以“之字形”光路传输的薄管激光,当光束为线偏振光时,其在不同方位角上的 p 偏振光与 s 偏振光分量不同,而全内反射对于 p 偏振光与 s 偏振光的附加相位存在差异。因此,对于无任何偏振调控的“之字形”光路薄管激光而言,线偏振光经过薄管激光增益介质后在每个方位角上的偏振态变得各不相同,致使其偏振态遭到严重破坏<sup>[19-20]</sup>。在两个薄管增益介质之间插入一个 90°旋光器后,薄管 1 中的 p 偏振光与 s 偏振光分量经过 90°旋光器后方向互易,致使薄管 1 中累积的相位差可通过薄管 2 得到补偿,从而恢复线偏振态。最后,通过  $\lambda/4$  波片控制往返光束线偏振方向,进而利用偏振分束镜实现注入光束与放大光束的分离<sup>[21-22]</sup>。

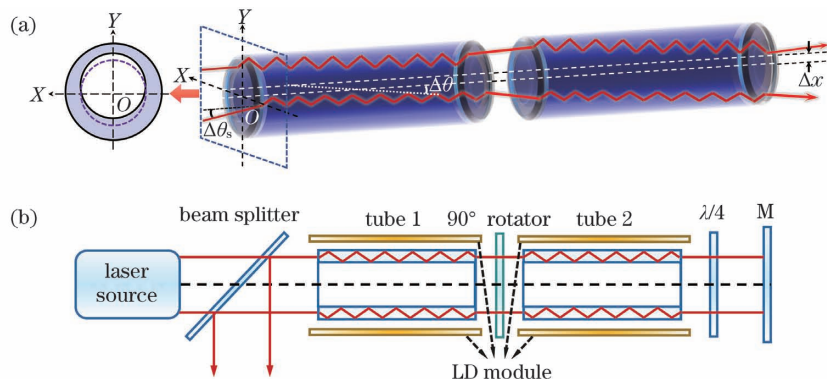


图 1 双管级联薄管激光放大器原理图。(a) 环域像差的产生;(b) 薄管激光器结构示意图

Fig. 1 Schematic diagram of two-stage tube laser amplifier. (a) Production of annular aberration;(b) schematic diagram of tube laser structure

为了校正静态误差引入的环域离轴像差,本文提出了一种基于共轭光路的双管级联薄管激光放大器环域像差自补偿方法,其基本思想是利用薄管构型中任意径向对称分布光路的光学共轭特性来实现环域低阶离轴像差的自补偿。图 2 为基于共轭光路的双管级联结构光束质量自补偿原理示意图。将两个抽运条件相同的激光晶体串接,中间设置 90°石英旋光器,使光束偏振方向旋转 90°,以补偿热应力导致的双折射效应<sup>[23-25]</sup>。直角内锥面反射镜的特殊结构使其具有平行回射特性,当准直光束沿光轴方向入射至圆锥斜面后,经圆锥内表面两次反射,出射

光束将以与入射光束平行的方向反向射出圆锥反射镜。不论入射光线方向如何改变,出射光线的方向始终与入射光线方向保持一致,且反射光线位置与入射光线位置以光轴对称<sup>[26-27]</sup>。基于直角锥镜的反射作用,激光束依次经过非理想双管级联薄管激光放大系统中任意一对光学共轭光路,将产生径向对称的像差分布,致使薄管激光经往返传输后,即可实现环域波前像差的自补偿。

本文采用光学分析软件 ASAP 对具有加工误差和对准误差的非理想薄管内的传输光线进行追迹,进而得到畸变波前分布  $\varphi_E$  为<sup>[28]</sup>

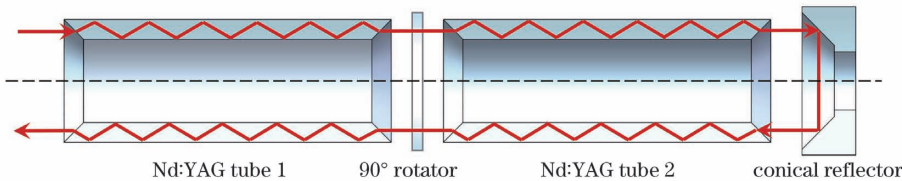


图2 双管级联薄管激光放大系统自补偿原理示意图

Fig. 2 Schematic diagram of configuration for correcting in two-stage tube laser amplifier with self-correction

$$\left\{ \begin{array}{l} \varphi_E = \int_{\text{beam path}} (n_0 \Delta L_{\text{OPL}}) ds \\ \Delta L_{\text{OPL}} = \int_{\text{real path}} (L_{\text{OPL1}}) ds_1 - \int_{\text{ideal path}} (L_{\text{OPL0}}) ds_0 \end{array} \right. , \quad (1)$$

式中: $L_{\text{OPL0}}$ 与 $L_{\text{OPL1}}$ 分别为室温条件下理想与非理想薄管内传输光线的光程; $n_0$ 是YAG在室温下的

折射率( $n_0=1.82$ ); $ds$ 为光线传输路径单元。

于是,薄管输出光场分布可表示为

$$E_1 = E_0 \exp(i k \varphi_E), \quad (2)$$

式中: $k=2\pi/\lambda$ , $\lambda$ 为光波长; $E_0$ 表示薄管输出激光的振幅分布。对于薄管输出的环形光束来说,可表示为<sup>[29]</sup>

$$E_0 = U_{01}(x_0, y_0) - U_{02}(x_0, y_0), \quad (3)$$

$$U_{01}(x_0, y_0) = \exp \left[ -\frac{(N+1)(x_0^2 + y_0^2)}{w_0^2} \right] \sum_{n=0}^N \frac{1}{n!} \left[ \frac{(N+1)(x_0^2 + y_0^2)}{w_0^2} \right]^n, \quad (4)$$

式中: $N$ 为平顶光束阶数; $w_0$ 和 $w'_0$ 分别为两束平顶光束对应的束宽。令 $w'_0 = \epsilon w_0$ , $\epsilon$ 为遮拦比, $0 < \epsilon < 1$ 。将(4)式中的 $w_0$ 换为 $w'_0$ 即为 $U_{02}$ 。

根据(1)~(4)式,可计算得到焦平面上的光场分布为

$$E = \frac{\exp(ikf)}{i\lambda f} \iint E_1(x_0, y_0) \cdot \exp \left\{ -\frac{ik}{f} (x_0 x_f + y_0 y_f) \right\} dx_0 dy_0. \quad (5)$$

采用 $\beta$ 因子对光束质量进行评价,其定义为<sup>[30]</sup>

$$\beta = \frac{r}{r_L}, \quad (6)$$

式中: $r_L$ 与 $r$ 分别为理想与实际环形光束在衍射极限下的焦斑半径。

### 3 自补偿方法效果分析

本文计算所采用的参数如下:直角锥镜基座材料为熔石英,反射面为镀有高反射膜系的内圆锥面,通光口直径为80 mm;激光波长 $\lambda=1064$  nm,薄管输出的窄带环形光束环宽为6 mm,内外环半径 $R_i$ 和 $R_o$ 分别为25.5 mm和31.5 mm,遮拦比 $\epsilon=0.810$ ;Nd: YAG的折射率为1.83,管内的临界反射角 $\gamma=33.69^\circ$ 。计算远场光束质量 $\beta$ 因子时所采用的聚焦透镜焦距 $f=500$  mm。

#### 3.1 双管级联薄管激光放大器自补偿效果分析

为便于讨论且不失一般性,在仿真时仅考虑

了单一误差对光束质量的影响。为了便于比较,本文还在双管结构的一端引入了平面反射镜,使薄管出射光束经平面镜反射后沿原路径返回管内逆向传输,以此作为双管级联薄管激光放大器自补偿效果分析的对照组。图3给出了当双管级联薄管激光放大器中仅管1分别存在同心度误差 $\Delta x$ 、平行度误差 $\Delta\theta$ 和光源对准误差 $\Delta\theta_s$ 时,自补偿前后 $\beta$ 值的变化及远场焦斑光强分布。从图3(a1)、(b1)与(c1)中可以看出,随着同心度误差 $\Delta x$ 、平行度误差 $\Delta\theta$ 和光源对准误差 $\Delta\theta_s$ 的增大,对照组(采用平面镜)的输出光束质量几乎呈线性关系迅速下降,而经自补偿后的输出光束质量则得到显著改善,其 $\beta$ 值约为1。从图3(a2)~(a8)、(b2)~(b8)与(c2)~(c8)中可以看出,远场焦斑形态随着同心度误差 $\Delta x$ 、平行度误差 $\Delta\theta$ 和光源对准误差 $\Delta\theta_s$ 的增大而发生严重畸变,特别是在误差较大时,焦斑分布呈现出明显的离轴趋势,表明畸变波前中所包含的环域离轴像差成分比例升高。然而,经校正后,焦斑形态均得到良好控制,能量分布更加集中。进一步分析图3(c6)~(c8)可知,对于光源对准误差 $\Delta\theta_s$ ,尽管焦斑形态得以校正,但其离轴趋势并未得到补偿。由此可见,本文提出的自补偿方法只能校正双管自身引入的离轴像差,而难以补偿光源倾斜入射时引入的倾斜角误差。

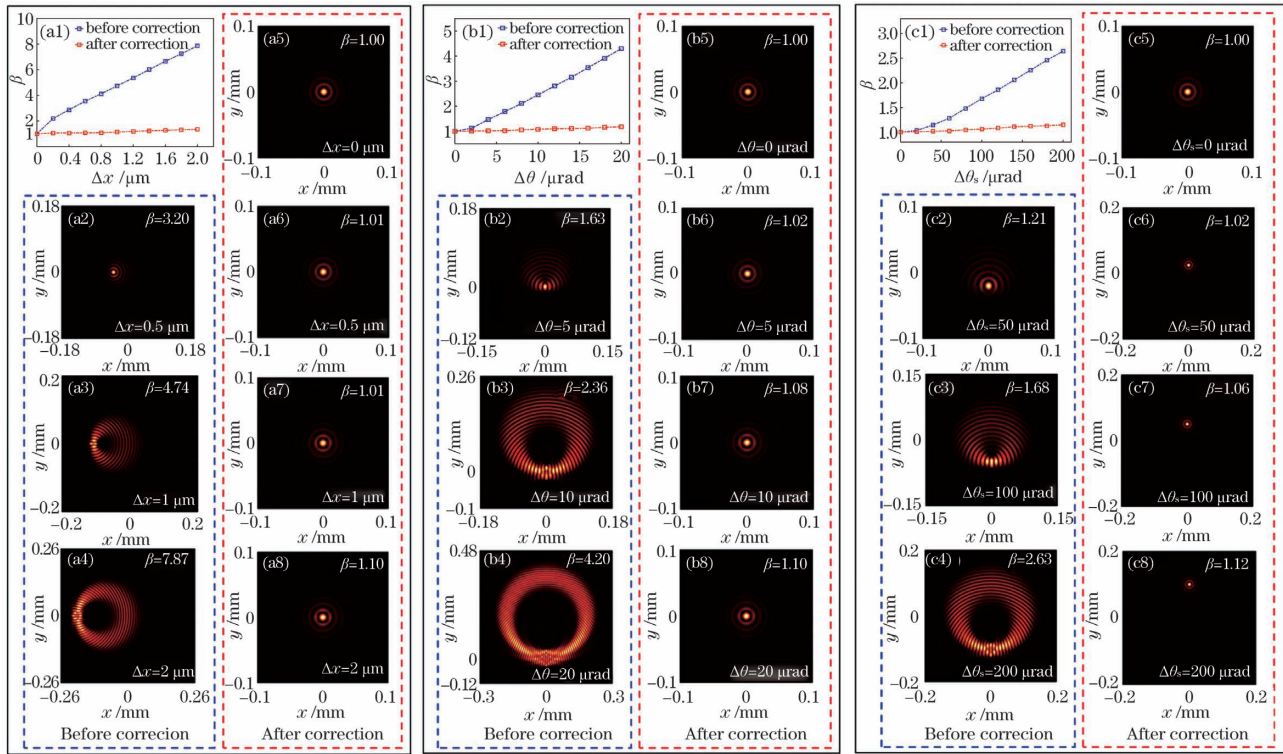


图 3 自补偿前后  $\beta$  值变化曲线与远场光强对比。(a1)~(a8)同心度误差;(b1)~(b8)平行度误差;(c1)~(c8)对准误差

Fig. 3 Comparison of the curves of  $\beta$  factor and far-field intensity distributions before and after self-correction.

(a1)~(a8) Concentricity error; (b1)~(b8) parallelism error; (c1)~(c8) collimation error

图 4 进一步给出了光源对准误差  $\Delta\theta_s = 1$  mrad 时,经补偿后的焦斑光强分布。虽然,由光源对准误差引起的离轴像差会导致自补偿后的焦斑偏离薄管轴线中心,但仍能够观察到较为理想的焦斑分布。进一步从远场光束质量来看,自补偿后的  $\beta$  值为

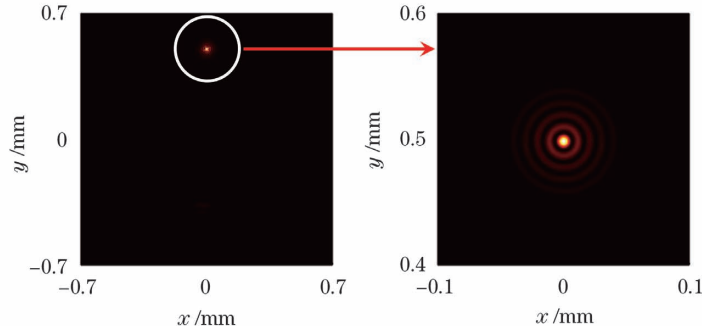


图 4 自补偿后焦面光强分布( $\Delta\theta_s = 1$  mrad)

Fig. 4 Intensity distribution with self-correction on the focal plane( $\Delta\theta_s = 1$  mrad)

为进一步说明上述静态误差引起的光束质量退化特性,本文基于环域 Zernike 多项式分解理论,分析了双管级联薄管激光放大器的波前像差特性<sup>[31]</sup>。环域 Zernike 多项式引入了新的变量——遮拦比  $\epsilon$ ,可用于环形光瞳系统的像差进行表征。在单位环形光瞳内,光场波前可表示为 Zernike 环域多项式的线性组合<sup>[32]</sup>,

1.25,表明基于共轭光路的自补偿方法对具有对准误差的畸变波前有显著的校正作用。由此可见,直角锥镜的引入能有效地扩展“之字形”光路双管级联薄管激光放大器的入射角度范围,使得本方法可以在一定范围内任意入射角度使用。

$$w(x, y, \epsilon) = \sum_{i=1}^N a_i Z_i(x, y, \epsilon), \quad (7)$$

式中: $w(x, y, \epsilon)$ 为波像差函数; $Z(x, y, \epsilon)$ 为第  $i$  阶 Zernike 多项式; $N$  为拟合阶数; $a_i$  为第  $i$  阶 Zernike 多项式系数。

图 5 给出了双管级联薄管激光放大器输出光束的波像差,图中同心度误差  $\Delta x = 1$   $\mu\text{m}$ ,平行度误差

$\Delta\theta=20 \mu\text{rad}$ , 光源对准误差  $\Delta\theta_s=100 \mu\text{rad}$ 。从图 5(a)中可以看出, 管 1 存在的同心度误差、平行度误差及光源对准误差均会导致倾斜与彗差等离轴像差。其中, 倾斜只会影响光束的传输方向, 但不会对光束质量产生明显影响, 而彗差则是降低光束质量的根本原因。彗差引发的轴外畸变会使远场焦斑分布表现出强烈的非中心对称弥散特性, 导致光束质量严重退化, 如图 3(a2)~(a4)、(b2)~(b4)、(c2)~(c4)所示。对比图 5(a)和(b)可知, 由同心度、平行度及光源对准误差导致的畸变波前, 其波前

峰谷(PV)值比未补偿时下降了近两个数量级, 表明该方法对环域低阶离轴像差具有良好的补偿作用。经补偿后, 远场焦斑分布接近理想焦斑, 光束质量显著提高, 如图 3(a6)~(a8)、(b6)~(b8)、(c6)~(c8)所示。当双管级联薄管激光放大器中仅管 2 分别存在同心度误差与平行度误差时, 其结果与管 1 一致。综上所述, 采用基于共轭光路的双管级联薄管激光放大器光束质量自补偿方法, 可有效抑制级联结构中任一薄管由装调误差及加工误差引起的环域离轴像差。

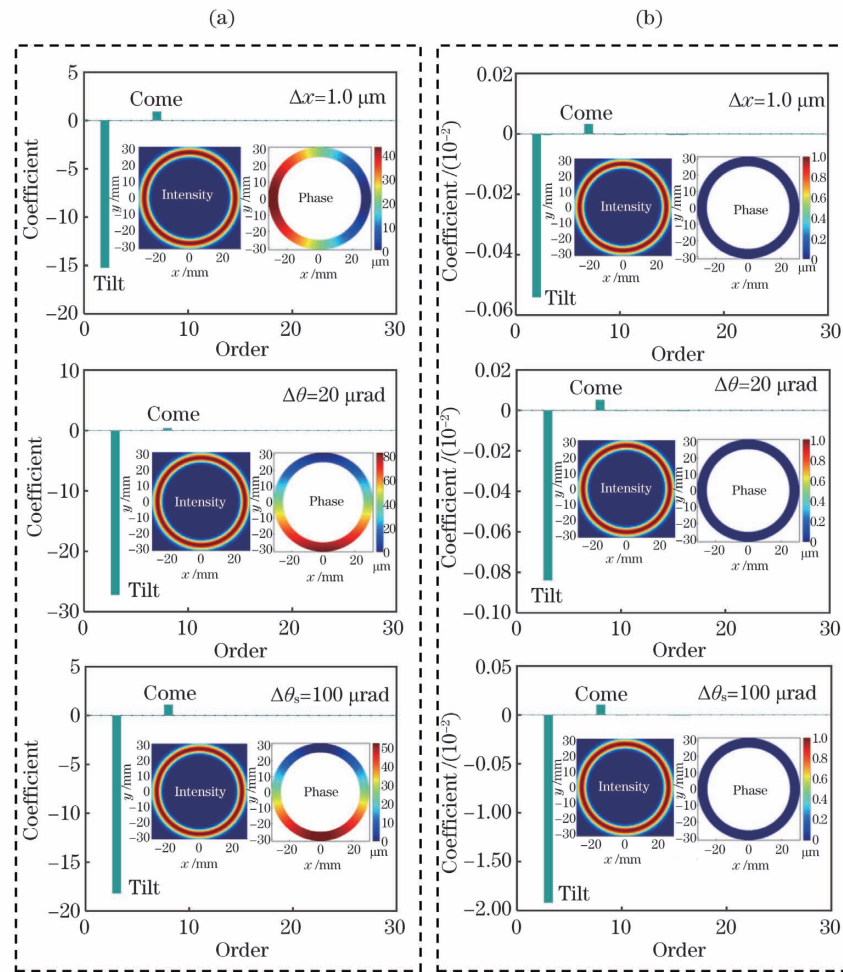


图 5 薄管激光波前像差分解图。(a)未补偿波前;(b)补偿后波前

Fig. 5 Wavefront aberration decomposition of tube laser. (a) Wavefront before correction; (b) wavefront after correction

### 3.2 自补偿方法对双管配合误差的补偿效果分析

与 3.1 节类似, 在分析自补偿方法对双管级联薄管激光放大器输出光束的自补偿效果时, 仿真过程仅考虑单一误差的作用。同时, 在无自补偿功能的双管级联结构中引入平面反射镜作为自补偿效果分析的对照组。本文以管 1 端面为  $XOY$  面、系统轴线方向为  $z$  轴建立柱坐标系。图 6 为双管级联薄管激光放大器的双管配合误差示意图。

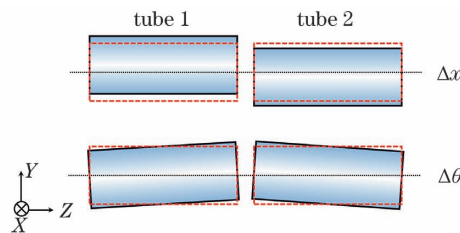


图 6 双管配合误差示意图

Fig. 6 Schematic diagram of matching error of two-stage tubes

表 1 列出了双管同时存在同心度配合误差时自补偿前后的光束质量对比结果。分析表 1 可知, 自补偿后的畸变波前 PV 值显著下降, 表明自补偿方法双管同心度配合误差引入的主要环域离轴像差(倾斜与彗差)具有很好的校正作用, 其光束质量得到显著改善。

表 1 同心度配合误差自补偿效果对比

Table 1 Comparison of self-correction effect before and after concentricity error

$\Delta x / \mu\text{m}$		Before correction		After correction	
Tube1	Tube2	$\beta$	PV / $\mu\text{m}$	$\beta$	PV / $\mu\text{m}$
0.3(X)	0.3(X)	4.15	13.30	1.07	0.06
0.3(X)	0.3(Y)	2.33	10.00	1.07	0.06
0.3(X)	-0.3(X)	1.08	0.08	1.00	$\approx 0$
0.5(Y)	-0.5(Y)	1.08	0.08	1.00	$\approx 0$
0.5(X)	0.5(Y)	5.93	25.60	1.07	0.06
0.5(X)	-0.3(X)	1.53	4.70	1.07	0.06
0.5(X)	-0.3(Y)	2.41	10.30	1.07	0.06

表 2 给出了双管级联薄管激光放大器存在平行度配合误差时补偿前后的光束质量对比结果。从表 2 可以看出, 经补偿后, 输出光束质量显著提高。

表 2 平行度配合误差自补偿效果对比

Table 2 Comparison of self-correction effect before and after parallelism error

$\Delta x / \mu\text{m}$		Before correction		After correction	
Tube1	Tube2	$\beta$	PV / $\mu\text{m}$	$\beta$	PV / $\mu\text{m}$
10(X)	0(X)	2.47	10.5	1.07	0.06
0(X)	10(X)	3.07	14.2	1.11	0.12
5(X)	-5(X)	2.20	8.9	1.10	0.11
5(X)	5(Y)	6.00	31.1	1.12	0.13
5(X)	-5(Y)	6.03	31.1	1.14	0.15

### 3.3 直角锥镜参数的影响分析

在实际补偿过程中, 通常难以达到直角锥镜与薄管的完美配准。为更好地改善光束质量, 有必要对直角锥镜的关键参数及其影响进行分析。

由于直角锥镜具有旋转对称性, 沿  $z$  轴方向的偏移与绕  $z$  轴的旋转均不会导致装调误差。直角锥

善。值得指出的是, 当双管分别引入与薄管激光放大系统轴线截面径向对称的同心度误差时, 其引发的波前畸变会相互抵消, 最终使光束质量大幅提升。分析其物理原因在于: 薄管内光束在传输过程中产生的波前相位畸变幅度相当、方向相反, 导致畸变自行消除。

与同心度误差不同的是, 双管平行度误差引起的波前畸变并不会因为沿系统轴线径向对称分布而发生抵消。

镜的装调误差分为平移误差, 即直角锥轴线相对于薄管轴线沿任意方向产生的偏移量  $\Delta l$ , 以及旋转误差, 即直角锥轴线相对于薄管轴线的偏转角度  $\Delta\alpha$ , 如图 7(a) 所示。在实际加工过程中, 因圆锥顶角很难达到严格  $90^\circ$ , 从而引入锥角误差, 如图 7(b) 所示。

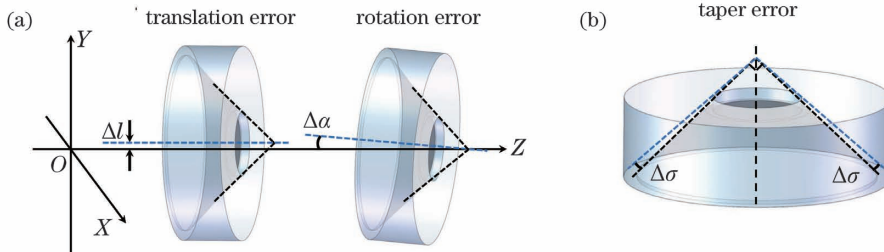


图 7 直角锥镜误差示意图。(a) 平移误差与旋转误差;(b) 锥角误差

Fig. 7 Schematic diagram of right-angle conical reflector errors. (a) Translation error and rotation error; (b) taper error

本文以较为敏感的薄管同心度误差为例,分析了双管级联薄管激光放大器中管 1 与管 2 分别存在  $0.5 \mu\text{m}$  的同向同心度误差时,非理想直角锥镜的补偿效果。图 8 给出了非理想直角锥镜补偿后的  $\beta$  值变化曲线及远场焦斑分布。

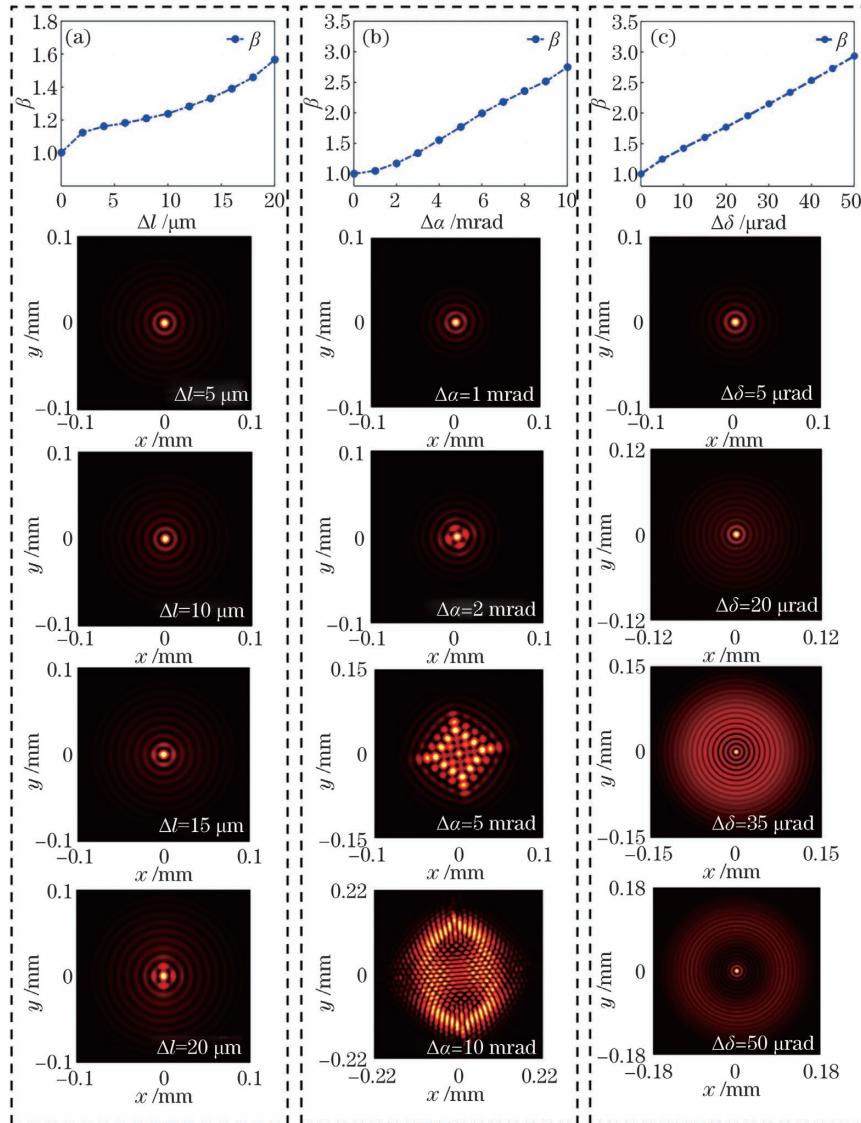


图 8 非理想锥镜补偿后  $\beta$  值变化曲线与远场光强分布。(a) 平移误差;(b) 旋转误差;(c) 锥角误差

Fig. 8 Curves of  $\beta$  factor and far-field intensity distributions after non-ideal cone lens compensation. (a) Translation errors; (b) rotation errors; (c) taper errors

从图 8(a)可以看出,当平移误差  $\Delta l < 10 \mu\text{m}$  时,  $\beta$  值随着平移误差  $\Delta l$  的增加而缓慢上升。然而,当其超过  $10 \mu\text{m}$  后,  $\beta$  值的增长幅度变大, 特别是超过  $20 \mu\text{m}$  时, 其远场焦斑图案出现明显形变, 说明直角锥镜平移误差对其补偿能力产生的负面影响加重。观察图 8(b)可知, 当旋转误差  $\Delta \alpha < 2 \text{ mrad}$  时,  $\beta$  值随着旋转误差  $\Delta \alpha$  的增大略有增长。然而, 当  $\Delta \alpha$  超过  $2 \text{ mrad}$  时, 输出光束质量迅速降低, 远场焦斑分布产生严重形变, 具体表现为焦斑形态以中心对称的形式弥散。由图 8(c)可

知, 随着锥角误差  $\Delta \delta$  增大,  $\beta$  值呈线性快速上升, 光束质量严重退化, 当  $\Delta \delta$  超过  $20 \mu\text{rad}$  时, 远场焦斑出现明显发散。

根据以上分析可知, 如果远场  $\beta$  值不出现明显增长, 则直角锥镜对平移误差  $\Delta l$  与旋转误差  $\Delta \alpha$  的容限分别可达数十微米量级与毫弧度量级, 而对锥角误差的容限仅为微弧度量级。由此可见, 本文提出的自补偿方法对装调误差的容限更高, 即该自补偿方法对装调误差具有更强的适应性, 而对加工误差十分敏感。在实际工作中, 为保证双管级联薄管

激光放大器输出光束的光束质量,应当对直角锥镜的加工误差进行重点管控。

为了进一步明确直角锥镜参数对波前相位的影响

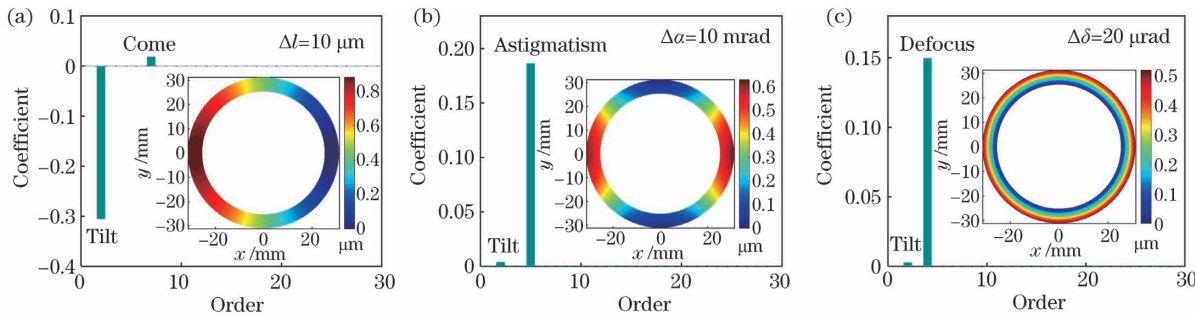


图9 薄管激光波前像差分解图。(a)平移误差  $10 \mu\text{m}$ ; (b)旋转误差  $10 \text{ mrad}$ ; (c)锥角误差  $20 \mu\text{rad}$

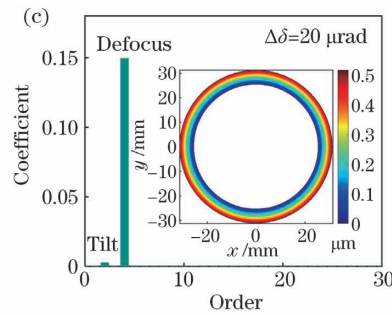
Fig. 9 Wavefront aberration decomposition of tube laser. (a) Translation error is  $10 \mu\text{m}$ ; (b) rotation error is  $10 \text{ mrad}$ ; (c) taper error is  $20 \mu\text{rad}$

由图9(a)~(c)可知,当直角锥镜平移误差、旋转误差和锥角误差分别为  $10 \mu\text{m}$ 、 $10 \text{ mrad}$  和  $20 \mu\text{rad}$  时,薄管输出环形光畸变波前 PV 值分别为  $0.88 \mu\text{m}$ 、 $0.63 \mu\text{m}$  和  $0.52 \mu\text{m}$ 。其中,平移误差主要引起环域倾斜( $n=2$ )与环域彗差( $n=7$ ),旋转误差主要引起环域像散( $n=5$ ),而锥角误差则主要引起环域离焦( $n=4$ )。总体而言,基于共轭光路的双管级联薄管激光放大器光束质量自补偿方法虽难以校正轴上像差,但可有效地补偿由装调误差与加工误差引起的主要环域离轴像差,在不增加系统冗余的同时显著提升薄管激光光束质量。

## 4 结 论

本文提出了一种适用于高功率双管级联薄管激光放大器环域像差的自补偿方法,可利用管状结构的径向光学共轭特性实现环域像差的自补偿。通过模拟计算验证了该自补偿方法校正双管结构误差与双管配合误差所产生畸变波前的有效性。结果表明,该方法对双管结构中任一薄管自身引入的同心度误差与平行度误差均有良好的校正作用,并能有效补偿双管配合误差引入的波前畸变,但对于光源引入的对准误差只能改善光束质量却无法校正其倾斜角。结果表明,该方法不仅可以显著提升双管级联激光放大器光束质量,还可扩展双管级联激光放大器的入射角范围,使得双管级联激光放大器能在一定范围内任意入射角度使用。本文方法使用的直角锥镜元件对装调误差容限较大,有利于工程应用。然而,在实际应用中,为保证该方法的自补偿效果,应对直角锥镜加工误差进行重点管控。

响,本文对薄管激光环域波前进行了分解。图9所示为双管级联薄管激光放大器输出波前的像差分析结果。



致谢 感谢中国科学院空间精密测量技术重点实验室为本文工作提供 ASAP (Advanced Systems Analysis Program) 软件支持。

## 参 考 文 献

- [1] Goodno G D, Komine H, McNaught S J, et al. Coherent combination of high-power, zigzag slab lasers[J]. Optics Letters, 2006, 31(9): 1247-1249.
- [2] Savich M. High power tube solid-state laser with zigzag propagation of pump and laser beam [J]. Proceedings of SPIE, 2015, 9342: 934216.
- [3] Jiang H, Chen X M, Xu L, et al. Quasi-continuous-wave, laser-diode-end-pumped Yb : YAG zigzag slab oscillator with high brightness at room temperature [J]. Applied Physics Express, 2017, 10 (2): 022702.
- [4] Kawashima T, Kanabe T, Matsui H, et al. Design and performance of a diode-pumped Nd: Silica-phosphate glass zig-zag slab laser amplifier for inertial fusion energy [J]. Japanese Journal of Applied Physics, 2001, 40(Part 1, No. 11): 6415-6425.
- [5] Li S G, Ma X H, Li H H, et al. Laser-diode-pumped zigzag slab Nd : YAG master oscillator power amplifier [J]. Chinese Optics Letters, 2013, 11(7): 071402.
- [6] Wittrock U, Weber H, Eppich B. Inside-pumped Nd : YAG tube laser[J]. Optics Letters, 1991, 16 (14): 1092-1094.
- [7] Tamida T, Nishimae J. Annular resonator with a Cassegrain configuration[J]. Applied Optics, 1997, 36(24): 5844-5848.
- [8] Wittrock U, Eppich B, Weber H. Beam quality of the 1-kW inside-pumped Nd : YAG tube laser[C]// Conference on Lasers and Electro-Optics, May 10-

- 15, 1992, Anaheim, California, United States. Washington D.C.: OSA, 1992: CTuE6.
- [9] Li X W, Yu C L, Shen H, et al. Thermo-optic effect and mode instability threshold characteristics of high-power fiber laser [J]. Chinese Journal of Lasers, 2019, 46(10): 1001001.  
李学文, 于春雷, 沈辉, 等. 高功率光纤激光热光效应及模式不稳定阈值特性研究 [J]. 中国激光, 2019, 46(10): 1001001.
- [10] Yang S D, Yin D J, Gan Z B, et al. Thermal effect of high energy repetition rate neodymium glass laser [J]. Chinese Journal of Lasers, 2020, 47(9): 0901004.  
杨思达, 印定军, 甘泽彪, 等. 高能量重复频率钕玻璃激光器的热效应实验研究 [J]. 中国激光, 2020, 47(9): 0901004.
- [11] Cho S, Jeong J, Hwang S, et al. Thermal lens effect model of Ti: sapphire for use in high-power laser amplifiers [J]. Applied Physics Express, 2018, 11(9): 092701.
- [12] Wang Y, Ogawa T, Wada S, et al. Analyses of birefringence compensation for a laser system with two tandem-set Nd : YAG rods and two coupling lenses [J]. Lasers in Engineering, 2012, 23(5): 323-340.
- [13] Chen Y J, Pang Y, Zhou T J, et al. Acousto-optic Q-switch Nd : YAG laser with 10-kHz repetition rate and 425.6 mJ pulse energy [J]. Chinese Journal of Lasers, 2019, 46(7): 0701005.  
陈月健, 庞毓, 周唐建, 等. 10 kHz, 425.6 mJ 声光调Q Nd : YAG 激光器 [J]. 中国激光, 2019, 46(7): 0701005.
- [14] Tian B Y, Zhong Z Q, Huang C, et al. Analysis on beam quality of solid-state tube MOPA system with zigzag beam path [J]. IEEE Photonics Journal, 2019, 11(2): 1-11.
- [15] Sun C, Wang D E, Deng X W, et al. Numerical analysis of a novel two-stage enlargement and adaptive correction approach for the annular aberration compensation [J]. Optics Express, 2019, 27(18): 25205-25227.
- [16] Tian B Y, Yu J C, Zhang B, et al. Theoretical study on beam quality and thermal stability in solid-state zigzag tube laser amplifier [J]. Optical Engineering, 2020, 59(7): 076104.
- [17] Wang Y, Liu B, Ye Z B, et al. High peak power and high beam quality fiber-solid hybrid amplification laser system [J]. Chinese Journal of Lasers, 2018, 45(4): 0401007.  
汪勇, 刘斌, 叶志斌, 等. 高峰值功率高光束质量光纤-固体混合放大激光系统 [J]. 中国激光, 2018, 45(4): 0401007.
- [18] Jiang M H, Li Q, Lei H, et al. A pulsed master-oscillator power-amplifier Nd : YAG laser with average power of 3000 W [J]. Chinese Journal of Lasers, 2011, 38(11): 1102006.  
姜梦华, 李强, 雷訇, 等. 平均功率 3000 W 的MOPA 脉冲 Nd : YAG 激光器 [J]. 中国激光, 2011, 38(11): 1102006.
- [19] Lapucci A, Ciofini M. Polarization state modifications in the propagation of high azimuthal order annular beams [J]. Optics Express, 2001, 9(12): 603-609.
- [20] Włodarczyk P, Pustelný S, Budker D. System for control of polarization state of light and generation of light with continuously rotating linear polarization [J]. The Review of Scientific Instruments, 2019, 90(1): 013110.
- [21] Zhang Y X, Gao C Q, Wang Q, et al. High-energy, stable single-frequency Ho : YAG ceramic amplifier system [J]. Applied Optics, 2017, 56(34): 9531-9535.
- [22] Wang R X, Yao B Q, Zhao B R, et al. Single-longitudinal-mode Ho : YVO<sub>4</sub> MOPA system with a passively Q-switched unidirectional ring oscillator [J]. Optics Express, 2019, 27(24): 34618-34625.
- [23] Dong Y T, Zhao Z G, Pan S Q, et al. Investigation of the TEM<sub>00</sub>-mode output character from LD side-pumped two Nd : YAG rods in laser resonator [J]. Chinese Journal of Lasers, 2010, 37(10): 2467-2471.  
董延涛, 赵智刚, 潘孙强, 等. LD 侧面抽运双棒串接 Nd : YAG 激光腔的基模输出特性研究 [J]. 中国激光, 2010, 37(10): 2467-2471.
- [24] Wang Y, Inoue K, Kan H, et al. Birefringence compensation of two tandem-set Nd : YAG rods with different thermally induced features [J]. Journal of Optics A: Pure and Applied Optics, 2009, 11(12): 125501.
- [25] Wang Y, Kan H, Ogawa T, et al. Optimization of two-lens coupling structure for a tandem-set solid-state laser system [J]. Journal of Optics, 2010, 12(8): 085702.
- [26] Li H Q, Cheng Z H. Output characteristics of right angle cone mirror cavity laser [J]. Chinese Optics Letters, 2005, 3(11): 650-652.
- [27] Ling D X, Wang H C, Huang X Y, et al. Analysis of a right-angle conical reflector resonator by the transfer matrix method [J]. Optik, 2014, 125(21): 6539-6542.
- [28] Shin J S, Cha Y H, Cha B H, et al. Simulation of the wavefront distortion and beam quality for a high-power zigzag slab laser [J]. Optics Communications, 1301006-9

- 2016, 380: 446-451.
- [29] Bagini V, Borghi R, Gori F, et al. Propagation of axially symmetric flattened Gaussian beams [J]. Journal of the Optical Society of America A, 1996, 13(7): 1385-1394.
- [30] Ji Z Y, Zhang X F. Fitting relationship between the beam quality  $\beta$  factor of high-energy laser and the wavefront aberration of laser beam [J]. Proceedings of SPIE, 2018, 10619: 106190J.
- [31] Mahajan B V N. Zernike annular polynomials and optical aberrations of systems with annular pupils [J]. Applied Optics, 1994, 33(34): 8125-8127.
- [32] Peng A H, Ye H W, Li X Y, et al. 2D lateral shearing wave-front reconstruction based on decoupling difference zernike future defining coefficient method [J]. Acta Optica Sinica, 2011, 31(8): 0801001.
- 彭爱华, 叶红卫, 李新阳, 等. 基于解耦差分泽尼克待定系数法的二维横向剪切波面重建算法 [J]. 光学学报, 2011, 31(8): 0801001.

## Method for Self-Correction of Annular Off-Axis Aberrations in Two-Stage Tube Laser Amplifiers

Li Jia, Tian Boyu, Yu Jiangchuan, Zhang Bin\*

*College of Electronics and Information Engineering, Sichuan University, Chengdu, Sichuan 610064, China*

### Abstract

**Objective** Solid-state lasers have attracted extensive attention because of their advantages of high efficiency and high beam quality. Solid-state tube lasers with zigzag beam paths (SSZTLs) combine the outstanding characteristics of rod and slab lasers, such as compact structure and light weight, and overcome the shortcoming of insufficient thermal load capacity, providing a potential approach to realize high-power lasers. These advantageous characteristics have resulted in some attractive applications in the fields of military defense and industrial manufacturing. However, the beam quality of SSZTLs is extremely sensitive to alignment and fabrication errors of the gain medium owing to their unique tubular structure. To improve the beam quality of SSZTLs, we propose a novel self-correction method to eliminate annular off-axis aberrations of the laser beam in SSZTLs.

**Methods** Taking neodymium-doped yttrium aluminum garnet (Nd : YAG) two-stage tube laser amplifiers as an example, a novel beam-correction method based on a right-angled conical reflector was proposed for the self-correction of annular off-axis aberrations in high-power two-stage thin-walled tube laser amplifiers. A right-angled conical reflector makes the laser beam propagate through two conjugate beam paths successively, which compensates the off-axis aberrations. First, based on a numerical simulation, the validity of this method to correct fabrication and alignment errors of a single tube was verified. Then, the correction effect of this method on matching errors of two-stage tubes was further analyzed. Finally, the influence of the structural parameters of the right-angled conical reflector on the aberration correction effect was discussed and the wavefront aberration caused by alignment and fabrication errors of the right-angled conical reflector was quantitatively analyzed using the annular Zernike polynomial decomposition theory.

**Results and Discussions** The proposed self-correction method can effectively correct alignment and fabrication errors induced by a single tube medium. For tube media with concentricity, parallelism, and alignment errors, the output beam quality of SSZTLs with planar mirrors degrades rapidly and almost linearly with an increase in these errors. The output beam quality after correction is significantly improved, and the energy concentration of the focal spot becomes better (Fig. 3). In addition, for alignment error, although the focal spot distribution is well focused after correction, its off-axis tendency is not corrected. When the alignment error is large, the focal spot distribution shows an obvious off-axis tendency, but the ideal focal spot distribution can still be obtained. The self-correction method can only correct the off-axis aberration induced by two-stage tubes and contributes little to the correction of input beam inclination angles [Figs. 3(c6)-(c8) and Fig. 4]. To further illustrate beam quality degradation characteristics, laser beam aberrations were analyzed using the annular Zernike polynomial decomposition theory of wavefront aberration. As shown in Fig. 5, irrespective of the type of error considered, the main aberrations are tilt and coma and the peak valley (PV) of off-axis aberrations decreases by about two orders of magnitude compared with

those in two-stage tubes without self-correction (Fig. 5). In addition, the proposed method can effectively correct the matching errors of two-stage tubes. When concentricity and parallelism matching errors exist in the two-stage tubes, the PV of the wavefront distortion decreases dramatically (Tables 1 and 2).

Since achieving perfect assembly of the right-angled conical reflector and two-stage tubes in actual corrections is difficult, analyzing the key parameters of the right-angled conical reflector and their effects is necessary. Taking the sensitive concentricity error as an example, the correction effects of a non-ideal right-angled conical reflector were analyzed. When the right-angled conical reflector has translation, rotation, and taper errors tolerance for the translation and rotation errors can reach tens of microns and milliradians, respectively, while that for taper error is only microradians. Therefore, the proposed method has high tolerance for alignment errors and is highly sensitive to fabrication errors (Fig. 8). To further illustrate the effects of alignment and fabrication errors of the right-angled conical reflector on wavefront phase, laser beam aberrations were analyzed using the annular Zernike polynomials decomposition theory. Results show that the main components of translation error are tilt and coma, rotation error mainly induces astigmatism, and taper error primarily results in defocus (Fig. 9).

**Conclusions** In this paper, we proposed a self-correction method for the annular aberrations of high-power two-stage tube laser amplifiers. The simulation results validate the self-correction method in correcting alignment and fabrication errors of a single tube as well as matching errors of two-stage tubes. The proposed method can significantly eliminate the distortion wavefront caused by concentricity and parallelism errors of a single tube and the matching errors of two-stage tubes. However, the proposed method fails to compensate for the tilt aberration caused by alignment error. In conclusion, the proposed method not only dramatically improves the beam quality of two-stage tube laser amplifiers but also expands the range of incident angles for the input beam. Moreover, the right-angled conical reflector used in this work has a large tolerance for alignment errors, which is beneficial for engineering applications. In practical applications, to ensure the availability of the self-correction method, controlling fabrication errors of the right-angled conical reflector is necessary.

**Key words** lasers; two-stage tube laser amplifiers; right-angle conical reflector; self-correction; annular aberration

**OCIS codes** 140.3460; 010.3310